

## Three-Body Model Analysis of Subbarrier $\alpha$ Transfer Reaction

Tokuro FUKUI,<sup>1\*)</sup> Kazuyuki OGATA,<sup>1\*\*)</sup> and Masanobu YAHIRO<sup>1</sup>

<sup>1</sup>*Department of Physics, Kyushu University, Fukuoka 812-8581, Japan*

Subbarrier  $\alpha$  transfer reaction  $^{13}\text{C}(^6\text{Li}, d)^{17}\text{O}(6.356 \text{ MeV}, 1/2^+)$  at 3.6 MeV is analyzed with a  $\alpha + d + ^{13}\text{C}$  three-body model, and the asymptotic normalization coefficient (ANC) for  $\alpha + ^{13}\text{C} \rightarrow ^{17}\text{O}(6.356 \text{ MeV}, 1/2^+)$ , which essentially determines the reaction rate of  $^{13}\text{C}(\alpha, n)^{16}\text{O}$ , is extracted. Breakup effects of  $^6\text{Li}$  in the initial channel and those of  $^{17}\text{O}$  in the final channel are investigated with the continuum-discretized coupled-channels method (CDCC). The former is found to have a large back-coupling to the elastic channel, while the latter turns out significantly small. The transfer cross section calculated with Born approximation to the transition operator, including breakup states of  $^6\text{Li}$ , gives  $(C_{\alpha^{13}\text{C}}^{17\text{O}^*})^2 = 1.03 \pm 0.29 \text{ fm}^{-1}$ . This result is consistent with the value obtained by the previous DWBA calculation.

### §1. Introduction

Transfer reactions below Coulomb barrier energies are known to be a powerful technique to determine asymptotic properties of the overlap between the initial and final state wave functions, essentially free from uncertainties associated with optical potentials and structural complexity of wave functions in the nuclear interior region.<sup>1)</sup> Recently, subbarrier  $\alpha$  transfer reactions have been used to indirectly measure cross sections of  $\alpha$ -induced reactions of astrophysical interest.<sup>2),3)</sup> In Ref. 2), Johnson and collaborators determined the reaction rate of  $^{13}\text{C}(\alpha, n)^{16}\text{O}$  by measuring the  $^{13}\text{C}(^6\text{Li}, d)^{17}\text{O}(6.356 \text{ MeV}, 1/2^+)$  reaction; for simplicity, we henceforth denote the final state of  $^{17}\text{O}$  as  $^{17}\text{O}^*$ . The  $^{13}\text{C}(\alpha, n)^{16}\text{O}$  reaction is considered to be important as a neutron source for the slow neutron capture process (s-process) taken place in the asymptotic giant branch (AGB) stars.<sup>4)</sup>

In the cross section formula, Eq. (1) of Ref. 2), of the  $^{13}\text{C}(\alpha, n)^{16}\text{O}$  reaction based on  $R$ -matrix approach,<sup>5)</sup> the asymptotic normalization coefficient (ANC) for  $\alpha + ^{13}\text{C} \rightarrow ^{17}\text{O}^*$ ,  $C_{\alpha^{13}\text{C}}^{17\text{O}^*}$ , is the only missing quantity. Throughout this study we consider the ANC with Coulomb-modification,<sup>2)</sup> i.e., a value divided by the Gamma function  $\Gamma(2 + \eta)$ , where  $\eta$  is the Sommerfeld parameter for the  $\alpha$ - $^{13}\text{C}$  system. In Ref. 2), the  $\alpha$  transfer reaction  $^{13}\text{C}(^6\text{Li}, d)^{17}\text{O}^*$  was analyzed with DWBA, disregarding the breakup effects of  $^6\text{Li}$  and  $^{17}\text{O}^*$ , and  $(C_{\alpha^{13}\text{C}}^{17\text{O}^*})^2 = 0.89 \pm 0.23 \text{ fm}^{-1}$  was extracted. The ground state energy of  $^6\text{Li}$  is, however, just 1.47 MeV below the  $\alpha + d$  threshold. Furthermore, the binding energy of  $^{17}\text{O}^*$ , i.e.,  $^{17}\text{O}(6.356 \text{ MeV}, 1/2^+)$ , from the  $\alpha + ^{13}\text{C}$  threshold is only 3 keV. Therefore, to extract a reliable value of  $C_{\alpha^{13}\text{C}}^{17\text{O}^*}$ , one should investigate how important  $^6\text{Li}$  and  $^{17}\text{O}^*$  breakup are in the  $\alpha$  transfer reaction.

The purpose of the present Letter is to analyze the  $^{13}\text{C}(^6\text{Li}, d)^{17}\text{O}^*$  reaction at 3.6 MeV (for the incident energy of  $^6\text{Li}$ ) with the three-body ( $\alpha + d + ^{13}\text{C}$ ) model and

\*) E-mail: fukui@phys.kyushu-u.ac.jp

\*\*) Present address: Research Center for Nuclear Physics, Osaka University

to determine  $C_{\alpha^{13}\text{C}}^{17\text{O}^*}$  accurately. Roles of  ${}^6\text{Li}$  breakup in the initial channel and  ${}^{17}\text{O}$  breakup in the final channel are investigated with the continuum-discretized coupled-channels method (CDCC).<sup>6),7)</sup> As shown in §3.2, the former is found important as a large back-coupling to the elastic channel, while the latter is confirmed much less important. CDCC was proposed and developed by Kyushu group and has been highly successful in quantitatively reproducing observables of reaction processes in which virtual or real breakup effects of the projectile are significant.<sup>8),9)</sup> CDCC treats continuum states of the projectile nonperturbatively, with reasonable truncation and discretization, and thus can describe the breakup effects with very high accuracy. Note that theoretical foundation of CDCC was established in Refs. 10)–12). The transition from the  ${}^6\text{Li}+{}^{13}\text{C}$  channel to the  $d+{}^{17}\text{O}^*$  channel is described with Born approximation; the breakup states of  ${}^6\text{Li}$  are explicitly taken into account in the calculation of the transfer process. The ANC thus extracted is compared with the result of the previous DWBA analysis.

This paper is constructed as follows. In §2 we formulate the three-body wave functions in the initial and final channels and the transfer cross section of the  ${}^{13}\text{C}({}^6\text{Li}, d){}^{17}\text{O}^*$  reaction. Numerical setting is described in §3.1. Breakup effects of  ${}^6\text{Li}$  and  ${}^{17}\text{O}$  are investigated in §3.2, and the transfer cross section is analyzed and the ANC is extracted in §3.3. In §3.4 we see the convergence of the modelspace of CDCC, and in §3.5 we discuss the present result in comparison with the previous DWBA result. Finally, we give a summary in §4.

## §2. Formulation

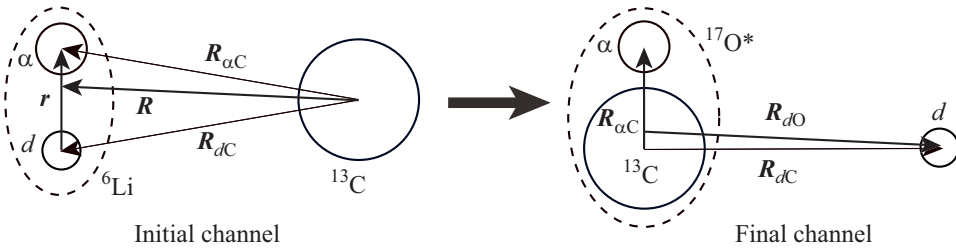


Fig. 1. Illustration of the three-body system in the initial and final channels.

In the present calculation, we work with the  $\alpha + d+{}^{13}\text{C}$  model shown in Fig. 1. The transition matrix ( $T$  matrix) for the transfer reaction  ${}^{13}\text{C}({}^6\text{Li}, d){}^{17}\text{O}^*$  is given by

$$T_{fi} = S_{\text{exp}}^{1/2} \langle \Psi_f^{(-)} | V_{\text{tr}} | \Psi_i^{(+)} \rangle, \quad (2.1)$$

where  $\Psi_i^{(+)}$  and  $\Psi_f^{(-)}$  are the three-body wave functions of the system in the initial and final channels, respectively, and  $V_{\text{tr}}$  is the transition operator of the transfer process. We put a normalization constant  $S_{\text{exp}}^{1/2}$  in  $T_{fi}$ , physics meaning of which is discussed below.

The three-body wave function  $\Psi_i^{(+)}$  in the initial state satisfies the Schrödinger

equation

$$(H_i - E)\Psi_i^{(+)}(\mathbf{r}, \mathbf{R}) = 0, \quad (2.2)$$

where  $E$  is the total energy of the system in the center-of-mass (c.m.) frame and  $\mathbf{r}$  ( $\mathbf{R}$ ) is the coordinate of  $\alpha$  ( ${}^6\text{Li}$ ) relative to  $d$  ( ${}^{13}\text{C}$ ). The Hamiltonian  $H_i$  is given by

$$H_i = T_{\mathbf{R}} + V_{d\text{C}}^{(\text{N})}(R_{d\text{C}}) + V_{\alpha\text{C}}^{(\text{N})}(R_{\alpha\text{C}}) + V^{\text{Coul}}(R) + h_i, \quad (2.3)$$

where  $T_{\mathbf{R}}$  is the kinetic energy operator associated with  $\mathbf{R}$  and  $h_i$  is the internal Hamiltonian of  ${}^6\text{Li}$ . We use  $V_{\text{XY}}^{(\text{N})}$  for the nuclear interaction between X and Y; each of X and Y represents a particle, i.e.,  $d$ ,  $\alpha$ , or C ( ${}^{13}\text{C}$ ). Similarly,  $\mathbf{R}_{\text{XY}}$  denotes the relative coordinate between X and Y.  $V^{\text{Coul}}$  is the Coulomb interaction between  ${}^6\text{Li}$  and  ${}^{13}\text{C}$ . Note that we neglect the Coulomb breakup of  ${}^6\text{Li}$ , which can be justified by the fact that the effective charge of the  $\alpha + d$  system for electric dipole transition is almost zero. Furthermore, as shown in §3.2, it is numerically confirmed that Coulomb breakup processes due to electric quadrupole and higher multipoles are negligibly small.

As the partial wave  $\Psi_{i;JM}$  of  $\Psi_i^{(+)}$ , we adopt the following CDCC wave function:

$$\Psi_{i;JM}^{\text{CDCC}}(\mathbf{r}, \mathbf{R}) = \sum_{j=0}^{j_{\max}} \sum_{\ell=0}^{\ell_{\max}} \sum_{L=|J-\ell|}^{J+\ell} \frac{\hat{\phi}_{j,\ell}(r)}{r} \frac{\hat{\chi}_{j,\ell,L}^J(R)}{R} \left[ i^\ell Y_\ell(\hat{\mathbf{r}}) \otimes i^L Y_L(\hat{\mathbf{R}}) \right]_{JM}, \quad (2.4)$$

where  $J$  and  $M$  are the total angular momentum and its  $z$ -component, respectively, and  $\ell$  ( $L$ ) is the orbital angular momentum between  $\alpha$  and  $d$  ( ${}^6\text{Li}$  and  ${}^{13}\text{C}$ ). We disregard the intrinsic spin of each particle for simplicity. The radial part of the  ${}^6\text{Li}$  wave function is denoted by  $\hat{\phi}_{j,\ell}(r)/r$ , where  $j$  is the energy index;  $j = 0$  corresponds to the ground state and  $j \neq 0$  to discretized continuum states obtained by the momentum-bin discretization.<sup>6)</sup> The internal wave function  $\hat{\Phi}_{j,\ell,m}$  given by

$$\hat{\Phi}_{j,\ell,m}(\mathbf{r}) = \frac{\hat{\phi}_{j,\ell}(r)}{r} i^\ell Y_{\ell m}(\hat{\mathbf{r}}) \quad (2.5)$$

satisfies

$$\left\langle \hat{\Phi}_{j',\ell',m'}(\mathbf{r}) | h_i | \hat{\Phi}_{j,\ell,m}(\mathbf{r}) \right\rangle = \epsilon_{j,\ell} \delta_{j'j} \delta_{\ell'\ell} \delta_{m'm}. \quad (2.6)$$

Inserting Eqs. (2.3) and (2.4) into Eq. (2.2) and making use of Eq. (2.6), one obtains the following CDCC equation:

$$\left[ -\frac{\hbar^2}{2\mu} \frac{d^2}{dR^2} + \frac{\hbar^2}{2\mu} \frac{L(L+1)}{R^2} + V^{\text{Coul}}(R) - E_{j,\ell} \right] \hat{\chi}_c^J(R) = - \sum_{cc'} F_{cc'}(R) \hat{\chi}_{c'}^J(R), \quad (2.7)$$

where  $\mu$  is the reduced mass of the  ${}^6\text{Li}$ - ${}^{13}\text{C}$  system,  $E_{j,\ell} = E - \epsilon_{j,\ell}$ , and

$$F_{cc'}(R) = \left\langle \frac{\hat{\phi}_{j',\ell'}(r)}{r} \left[ i^{\ell'} Y_{\ell'} \otimes i^{L'} Y_{L'} \right]_{JM} \left| V_{d\text{C}}^{(\text{N})} + V_{\alpha\text{C}}^{(\text{N})} \right| \frac{\hat{\phi}_{j,\ell}(r)}{r} \left[ i^\ell Y_\ell \otimes i^L Y_L \right]_{JM} \right\rangle_{\mathbf{r}, \hat{\mathbf{R}}}. \quad (2.8)$$

For simple notation, we denote the channel indices  $\{j, \ell, L\}$  as  $c$ . The CDCC equation is solved numerically up to  $R = R_{\max}$  and  $\hat{\chi}_c$  is connected with the usual boundary condition

$$\hat{\chi}_c^J(R) \rightarrow \begin{cases} U_{L,\eta_{j,\ell}}^{(-)}(K_{j,\ell}R)\delta_{cc_0} - \sqrt{K_{0,\ell_0}/K_{j,\ell}}\hat{S}_{cc_0}^J U_{L,\eta_{j,\ell}}^{(+)}(K_{j,\ell}R) & \text{for } E_{j,\ell} \geq 0 \\ -\hat{S}_{cc_0}^J W_{-\eta_{j,\ell},L+1/2}(-2iK_{j,\ell}R) & \text{for } E_{j,\ell} < 0 \end{cases}, \quad (2.9)$$

where  $K_{j,\ell} = \sqrt{2\mu E_{j,\ell}}/\hbar$ ,  $U_{L,\eta_{j,\ell}}^{(-)}$  ( $U_{L,\eta_{j,\ell}}^{(+)}$ ) is the incoming (outgoing) Coulomb wave function with the Sommerfeld parameter  $\eta_{j,\ell}$ , and  $W_{-\eta_{j,\ell},L+1/2}$  is the Whittaker function. The subscript 0 of  $\ell$  and  $c$  represents the incident channel. With the  $S$ -matrix elements  $\hat{S}_{cc_0}^J$  in Eq. (2.9), one may obtain any physics quantities with the standard procedure except that one needs to make the discrete results smooth when breakup observables are investigated.

Since the CDCC wave function  $\Psi_i^{\text{CDCC}}$  can be regarded as, with very high accuracy, an exact solution to Eq. (2.2) in evaluation of  $T$ -matrix elements that contain a short range interaction, one may define  $V_{\text{tr}}$  by

$$V_{\text{tr}} = V_{\alpha d}(r) + V_{dC}(R_{dC}) + V_{\alpha C}(R_{\alpha C}) - V_{\text{aux}} \quad (2.10)$$

with any choice of the auxiliary potential  $V_{\text{aux}}$ . In Eq. (2.10),  $V_{\alpha d}$ ,  $V_{dC}$ , and  $V_{\alpha C}$  contain both nuclear and Coulomb parts. Note that  $V_{\text{aux}}$  determines the final state wave function  $\Psi_f^{(-)}$ . In the present study, we adopt

$$V_{\text{aux}} = V_{dC}(R_{dC}) + V_{\alpha C}(R_{\alpha C}) + V_{\alpha d}^{(C)}(r), \quad (2.11)$$

which trivially gives

$$V_{\text{tr}} = V_{\alpha d}^{(N)}(r). \quad (2.12)$$

The superscript (C) of  $V_{\alpha d}$  in Eq. (2.11) represents the Coulomb part of the interaction. We then have

$$(H_f - E)\Psi_f^{(+)}(\mathbf{R}_{\alpha C}, \mathbf{R}_{dO}) = 0 \quad (2.13)$$

with

$$H_f = T_{\mathbf{R}_{dO}} + V_{dC}(R_{dC}) + V_{\alpha d}^{(C)}(r) + h_f, \quad (2.14)$$

where  $T_{\mathbf{R}_{dO}}$  is the kinetic energy regarding  $\mathbf{R}_{dO}$  and  $h_f$  is the internal Hamiltonian of  $^{17}\text{O}$ . Note that we here consider a Schrödinger equation for  $\Psi_f^{(+)}$ , which is the time-reversal of  $\Psi_f^{(-)}$ .

One can easily obtain the form of  $\Psi_f^{(+)}$  based on CDCC,  $\Psi_f^{\text{CDCC}(+)}$ , just in the same way as in the initial channel, except that i) we should include Coulomb breakup of  $^{17}\text{O}$ , ii) we have no nuclear part of  $V_{\alpha d}$ , and iii) the bound state of  $^{17}\text{O}$  at 6.356 MeV is a p-wave that generates both monopole and quadrupole interactions between  $d$  and  $^{17}\text{O}$ ; the latter causes also change in the  $d$ - $^{17}\text{O}$  angular momentum that is called reorientation. Note that  $V_{dC}$  in Eq. (2.14) contains both nuclear and Coulomb parts, as mentioned above.

It is shown in §3.2 that  $^{17}\text{O}$  breakup channels have very small ( $\sim 5\%$ ) effects on the  $d$ - $^{17}\text{O}$  elastic scattering. Furthermore, the quadrupole interaction is found negligibly small (see Fig. 2). Then we can approximate

$$\Psi_f^{\text{CDCC}(-)} \approx \varphi_0(\mathbf{r})\xi_0^{(-)}(\mathbf{R}_{dO}) \equiv \Psi_f^{\text{1ch}(-)}, \quad (2.15)$$

where  $\varphi_0(\mathbf{r})$  is the relative wave function between  $\alpha$  and  $^{13}\text{C}$  in  $^{17}\text{O}^*$ , and  $\xi_0^{(-)}(\mathbf{R}_{dO})$  is the distorted wave function obtained by the single-channel calculation, in which both the breakup channels and the aforementioned quadrupole interaction are switched off.

In the calculation of  $T_{fi}$ , we make zero-range approximation; the strength  $D_{j,\ell}$  of the zero-range  $\alpha$ - $d$  interaction is given by

$$D_{j,\ell} = \int \hat{\phi}_{j,\ell}^*(r) V_{\alpha d}^{(N)}(r) \hat{\phi}_{j,\ell}(r) dr. \quad (2.16)$$

The finite-range correction to the zero-range calculation of  $T_{fi}$  is made with the standard prescription.<sup>1)</sup> One may examine the validity of this approximation by the magnitude of the correction. We use  $\Psi_i^{(+)}$  calculated with CDCC, while  $\Psi_f^{\text{1ch}(-)}$  of Eq. (2.15) is adopted as  $\Psi_f^{(-)}$ , in the evaluation of  $T_{fi}$ .

### §3. Results and discussion

#### 3.1. Numerical input

The  $\alpha$ - $d$  wave function in  $\Psi_i^{\text{CDCC}}$  is constructed by following Ref. 13), except that we do not use the orthogonal condition model (OCM) but exclude Pauli's forbidden states by hand. We include  $\ell = 0, 1$ , and 2 states. As for the nuclear part of the  $\alpha$ - $d$  interaction for  $\ell = 0$ , we use

$$V_{\alpha d; \ell=0}^{(N)}(r) = -105.5 \exp[-(r/2.191)^2] + 46.22 \exp[-(r/1.607)^2]. \quad (3.1)$$

For  $\ell = 2$ ,

$$V_{\alpha d; \ell=2}^{(N)}(r) = -85.00 \exp[-(r/2.377)^2] + 30.00 \exp[-(r/1.852)^2] \quad (3.2)$$

is adopted. We neglect the intrinsic spin  $S$  of  $d$ , and we have only one resonance state at 3.474 MeV (measured from the ground state energy) with a width of 0.45 MeV. It is found that, however, if we include  $S$  and a spin-orbit interaction that reproduces the  $1^+$ ,  $2^+$ , and  $3^+$  resonance states, the resulting value of the ANC shown below changes by only 0.2%. Thus, the separation of the  $\ell = 2$  resonance state to  $1^+$ ,  $2^+$ , and  $3^+$  resonance states by the spin-orbit interaction plays no role in the present subbarrier  $\alpha$  transfer reaction. For  $\ell = 1$ , we adopt<sup>14)</sup>

$$V_{\alpha d}^{(N)}(r) = -74.19 \exp[-(r/2.236)^2], \quad (3.3)$$

which is used also for  $\ell > 2$  when we check the convergence of CDCC calculation with respect to  $\ell_{\text{max}}$  (see §3.4). The Coulomb interaction between  $\alpha$  and  $d$  is evaluated

by assuming a uniformly charged sphere with the charge radius  $R_C$  of 3.0 fm; see Eq. (3.5) below.

We take the maximum value  $k_{\max}(r_{\max})$  of the relative wave number  $k$  (coordinate  $r$ ) between  $\alpha$  and  $d$  to be  $2.0 \text{ fm}^{-1}$  (60 fm); the maximum relative energy  $\epsilon_{\max}$  is 62.4 MeV. We use  $j_{\max} = 100$  for each of the  $\ell = 0, 1,$  and  $2$  states and the width  $\Delta k$  of the momentum bin is thus  $0.02 \text{ fm}^{-1}$ . The number of channels,  $N_{\text{ch}}$ , in the CDCC equation (2.7) is 601. When we see the effects of Coulomb breakup in Fig. 2, we take  $r_{\max} = 300 \text{ fm}$ .

As for the interactions of the  $\alpha$ - $^{13}\text{C}$  and  $d$ - $^{13}\text{C}$  systems, we use the parameters shown in Table I. The standard Woods-Saxon form is adopted:

$$V(x) = -V_0 f_V(x) - iW_0 f_W(x) + V_C(x), \quad (3.4)$$

where  $f_V(x) = (1 + \exp[(x - R_V)/a_V])^{-1}$  and  $f_W(x) = (1 + \exp[(x - R_W)/a_W])^{-1}$ . The Coulomb interaction  $V_C(x)$  is given by

$$V_C(x) = \begin{cases} \frac{Z_1 Z_2 e^2}{2R_C} \left(3 - \frac{x^2}{R_C^2}\right) & x \leq R_C \\ \frac{Z_1 Z_2 e^2}{x} & x > R_C \end{cases}, \quad (3.5)$$

where  $Z_1 Z_2$  is the product of the atomic numbers of the interacting particles. These parameters are used in the calculation of both initial and final state wave functions. The parameter set for the  $d$ - $^{13}\text{C}$  system is determined to reproduce the elastic scattering cross section obtained with the parameters in Ref. 2) that contains a spin-orbit part. We determine  $V_0$  for the  $\alpha$ - $^{13}\text{C}$  system to reproduce  $\epsilon_0$  assuming that the orbital angular momentum is 1 and the number of forbidden states is 2. Note that we use Eq. (3.5) with  $R_C = 2.94 \text{ fm}$  for the  $^6\text{Li}$ - $^{13}\text{C}$  Coulomb interaction unless we include Coulomb breakup of  $^6\text{Li}$ .

Table I. Potential parameters used in the present calculation.

System	$V_0$ (MeV)	$R_V$ (fm)	$a_V$ (fm)	$W_0$ (MeV)	$R_W$ (fm)	$a_W$ (fm)	$R_C$ (fm)
$\alpha+^{13}\text{C}$	69.30	2.939	0.670	—	—	—	2.969
$d+^{13}\text{C}$	73.05	3.128	0.780	10.50	2.986	0.800	2.969

In the calculation of  $\Psi_{i;JM}^{\text{CDCC}}$ , we use  $R_{\max} = 15 \text{ fm}$  and  $J_{\max} = 7$ . Note that we explicitly include closed channels, in which  $E_{j,\ell} < 0$ , in CDCC calculations. In the evaluation of  $T_{fi}$ , we set the maximum value of  $R_{dC}$  to be 30 fm; we use the asymptotic form of  $\hat{\chi}_c^J$ , Eq. (2.9), to obtain  $\Psi_{i;JM}^{\text{CDCC}}$  for  $R > 15 \text{ fm}$ . When we include Coulomb breakup, we set  $R_{\max}$  to 200 fm.

For the final channel, the relative energy between  $\alpha$  and  $^{13}\text{C}$  in the  $1/2^+$  state at 6.356 MeV is  $\epsilon_0 = -3 \text{ keV}$  from the  $\alpha$ - $^{13}\text{C}$  threshold. In the calculation of  $\Psi_f^{\text{CDCC}(-)}$ , we include the p-wave bound state and the s-, p-, d-continua of the  $\alpha+^{13}\text{C}$  system up to the relative momentum of  $1.2 \text{ fm}^{-1}$  (relative energy of 39.6 MeV) with the momentum bin with a common width  $0.06 \text{ fm}^{-1}$ . The maximum values of  $R_{\alpha C}$  and

$R_{dO}$  are both set to 100 fm, and we put  $J_{\max} = 10$ . We include all closed channels in the CDCC calculations as in the initial channel.

### 3.2. Breakup effects of ${}^6\text{Li}$ and ${}^{17}\text{O}$

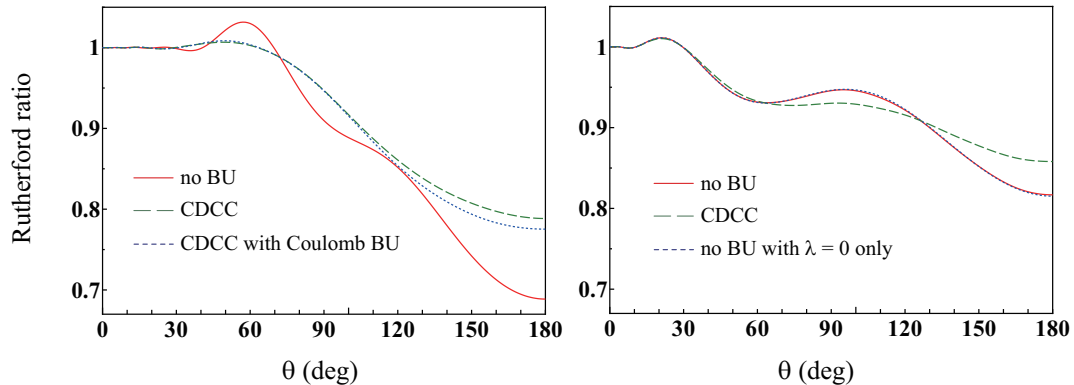


Fig. 2. (color online) Elastic cross sections of  ${}^6\text{Li}-{}^{13}\text{C}$  at 3.6 MeV (left panel) and  $d-{}^{17}\text{O}^*$  at 1.1 MeV (right panel). In each panel, the dashed line shows the result of CDCC and the solid line is the result without breakup channels. The dotted line in the left panel is the result of CDCC with both nuclear and Coulomb breakup, while that in the right panel shows the result without breakup including only the monopole interaction between  $d$  and  ${}^{17}\text{O}$ .

Figure 2 shows the elastic cross sections of  ${}^6\text{Li}-{}^{13}\text{C}$  at 3.6 MeV (left panel) and  $d-{}^{17}\text{O}^*$  at 1.1 MeV (right panel) corresponding to the initial and final channels, respectively, of the  ${}^{13}\text{C}({}^6\text{Li}, d){}^{17}\text{O}^*$  reaction. In each panel, the dashed line shows the result of CDCC and the solid line is the result without breakup channels. One sees from the left panel significant breakup effects on the elastic cross section, i.e., a large back-coupling to the elastic channel. Another finding is the inclusion of Coulomb breakup (the dotted line in the left panel) little affects the cross section. One can thus infer that nuclear breakup plays important roles in the  ${}^{13}\text{C}({}^6\text{Li}, d){}^{17}\text{O}^*$  reaction, and conclude that neglect of the Coulomb breakup in the calculation of  $\Psi_{i;JM}^{\text{CDCC}}$  is justified. On the other hand, in the final channel, effects of nuclear and Coulomb breakup are found very small as shown in the right panel; they change the cross section for  $\theta \gtrsim 60^\circ$  by 5% at most. We further investigate the breakup effects on the  $d-{}^{17}\text{O}^*$  wave function in the elastic channel. The absolute value (argument) of the wave function for  $J = 0$  at  $R_{dO} = 10$  fm, which is found to have the main contribution to the transfer amplitude, is 0.982 and 0.956 ( $278.8^\circ$  and  $276.7^\circ$ ) when the breakup states of  ${}^{17}\text{O}$  are included and neglected, respectively; the breakup effects are about 3%. Therefore, we can disregard the breakup channels of the  $d-{}^{17}\text{O}$  system in the calculation of  $T_{fi}$  with the error of 5% at most. The dotted line in the right panel shows the result with neglecting both the breakup channels and the quadrupole interaction between  $d$  and  ${}^{17}\text{O}$ , which is almost identical to the solid line. Thus, one can use Eq. (2.15) in the calculation of the final state wave function; we estimate the error due to this approximation to be 5% as mentioned above. It should be noted that breakup cross sections in the initial and final channels are both found smaller than the nuclear part of the elastic cross section by about four orders

of magnitude.

The very small breakup effects in the final channel are because the incoming energy of  $d$  is suitably below the Coulomb barrier, and the interaction that causes breakup in Eq. (2·14) is significantly weaker than in Eq. (2·3); note that  $V_{\alpha d}^{(N)}(r)$  is defined as  $V_{\text{tr}}$  and does not appear in Eq. (2·14).

### 3.3. Transfer cross section and ANC

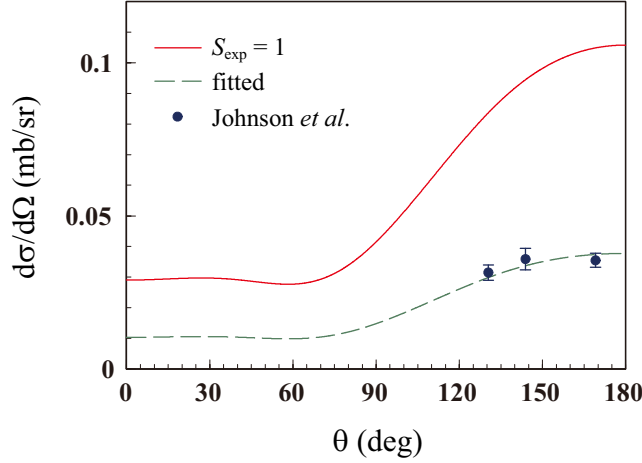


Fig. 3. (color online) Cross section of the transfer reaction  $^{13}\text{C}(^6\text{Li}, d)^{17}\text{O}^*$  at 3.6 MeV. The solid line is the result of calculation with  $S_{\text{exp}} = 1$ . The dashed line is the result of the  $\chi^2$  fit to the experimental data taken from Ref. 2).

We show in Fig. 3 the cross section of the transfer reaction  $^{13}\text{C}(^6\text{Li}, d)^{17}\text{O}^*$  at 3.6 MeV as a function of the outgoing angle  $\theta$  of  $d$  in the c.m. frame. The solid line represents the result with  $S_{\text{exp}} = 1$  and the dashed line shows the result of the  $\chi^2$  fit to the experimental data.<sup>2)</sup> The resulting value of  $S_{\text{exp}}$  is 0.357. Note that  $S_{\text{exp}}$  cannot be regarded as a spectroscopic factor. Indeed,  $S_{\text{exp}}$  has strong dependence on the model wave function of the  $\alpha$ - $^{13}\text{C}$  system; typically, it varies by a factor of 2 with changing the geometric parameters of  $V_{\alpha\text{C}}^{(N)}$  by 30%. This clearly shows that it is not feasible to determine  $S_{\text{exp}}$  from the present analysis of the experimental data. On the other hand, the ANC  $C_{\alpha^{13}\text{C}}^{17\text{O}^*}$  given by

$$C_{\alpha^{13}\text{C}}^{17\text{O}^*} = S_{\text{exp}}^{1/2} C_{\alpha^{13}\text{C}}^{\text{sp}} \quad (3\cdot6)$$

with the single particle ANC  $C_{\alpha^{13}\text{C}}^{\text{sp}}$  of the  $\alpha$ - $^{13}\text{C}$  wave function, is robust against changes in the potential parameters. This shows that the reaction process considered is peripheral with respect to  $R_{\alpha\text{C}}$ , i.e., only the tail of the  $\alpha$ - $^{13}\text{C}$  wave function contributes to the transition amplitude. Note that  $C_{\alpha^{13}\text{C}}^{\text{sp}}$  is defined by

$$C_{\alpha^{13}\text{C}}^{\text{sp}} = \frac{R_{\alpha\text{C}} \bar{\varphi}_0(R_{\alpha\text{C}})}{W_{-\bar{\eta}, 3/2}(2\kappa_0 R_{\alpha\text{C}}) \Gamma(2 + \bar{\eta})} \quad \text{at } R_{\alpha\text{C}} \gg R_N, \quad (3\cdot7)$$

where  $\bar{\varphi}_0$  is the radial part of  $\varphi_0$ ,  $\bar{\eta}$  is the Sommerfeld parameter of the  $\alpha$ - $^{13}\text{C}$  system,

$\kappa_0 = \sqrt{-2\mu_{\alpha^{13}\text{C}}\varepsilon_0}/\hbar$  with  $\mu_{\alpha^{13}\text{C}}$  the reduced mass of  $\alpha$  and  $^{13}\text{C}$ ,  $\Gamma$  is the Gamma function, and  $R_N$  represents the range of  $V_{\alpha\text{C}}^{(N)}$ .

The value of  $(C_{\alpha^{13}\text{C}}^{17\text{O}^*})^2$  extracted by the present calculation is  $1.03 \text{ fm}^{-1}$ . We then evaluate the uncertainty of  $(C_{\alpha^{13}\text{C}}^{17\text{O}^*})^2$  associated with the  $\alpha$ - $^{13}\text{C}$  and  $d$ - $^{13}\text{C}$  potential parameters shown in Table I by changing each value by 30%. Note that  $V_0$  for  $\alpha$ - $^{13}\text{C}$  has a constraint that it must reproduce  $\varepsilon_0$ . The uncertainty is found to be 22%. We take into account also the uncertainty due to the use of Eq. (2.15) (5%) and that coming from the zero-range approximation to  $V_{\alpha d}^{(N)}$  (8%), and conclude that the theoretical uncertainty is totally 24%. Including the ambiguity of experimental information<sup>2)</sup> together, we finally obtain

$$(C_{\alpha^{13}\text{C}}^{17\text{O}^*})^2 = 1.03 \pm 0.25 \text{ (theor)} \pm 0.15 \text{ (expt)}, \quad (3.8)$$

where (theor) and (expt) respectively represent theoretical and experimental uncertainties.

#### 3.4. Convergence of the CDCC wave function in the initial channel

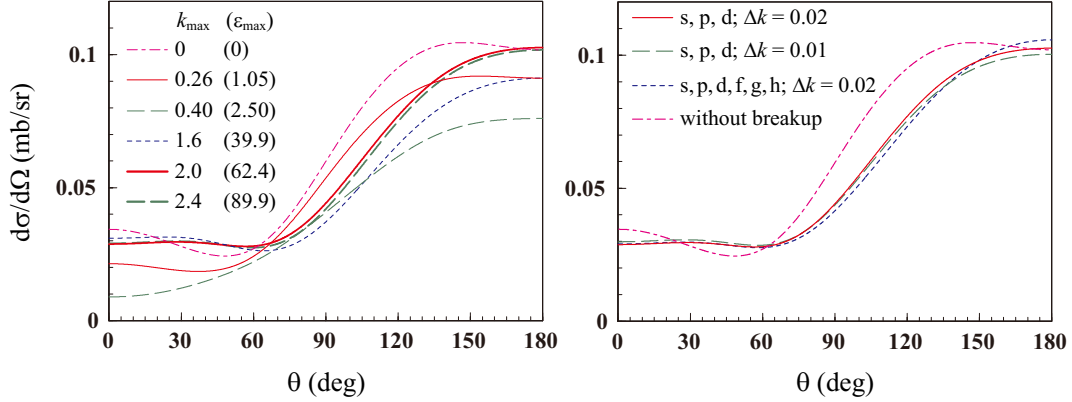


Fig. 4. (color online) The dependence the cross section for  $^{13}\text{C}(^6\text{Li}, d)^{17}\text{O}^*$  at 3.6 MeV on the modelspace of CDCC for  $\Psi_i^{\text{CDCC}}$ . In the left panel,  $k_{\text{max}}$  is varied. The values of  $k_{\text{max}}$  are shown in unit of  $\text{fm}^{-1}$  and the corresponding values of  $\varepsilon_{\text{max}}$  are given in the parentheses in unit of MeV. Here, the  $\ell = 0, 1$ , and  $2$  breakup continua are taken with  $\Delta k = 0.02 \text{ fm}^{-1}$ . In the right panel, the dashed line stands for the result of the  $\ell = 0, 1$ , and  $2$  breakup continua with  $k_{\text{max}} = 2.0 \text{ fm}^{-1}$  and  $\Delta k = 0.01 \text{ fm}^{-1}$ . The dotted line shows the result of the  $0 \leq \ell \leq 5$  continua with  $k_{\text{max}} = 2.0 \text{ fm}^{-1}$  and  $\Delta k = 0.02 \text{ fm}^{-1}$ . The thick solid line (the solid line) in the left (right) panel is the result of the  $\ell = 0, 1$ , and  $2$  breakup continua with  $k_{\text{max}} = 2.0 \text{ fm}^{-1}$  and  $\Delta k = 0.02 \text{ fm}^{-1}$  and the same as the solid line in Fig. 3. The result without breakup channels is also shown by the dash-dotted line in each panel.

Figure 4 shows the dependence of the cross section for  $^{13}\text{C}(^6\text{Li}, d)^{17}\text{O}^*$  at 3.6 MeV on the modelspace of CDCC for  $\Psi_i^{\text{CDCC}}$ . In the left panel, we show the convergence of the cross section with respect to increasing  $k_{\text{max}}$ , where the  $\ell = 0, 1$ , and  $2$  breakup continua are taken with  $\Delta k = 0.02 \text{ fm}^{-1}$ . One can see that the convergence is very slow and obtained at  $k_{\text{max}} = 2.0 \text{ fm}^{-1}$ . In usual CDCC calculation, one takes only the open channels, i.e., channels with  $E_{j,\ell} > 0$ . The result thus obtained (the thin

solid line) is, however, sizably different from the converged one (the thick dotted line), at backward angles in particular. Thus, inclusion of the breakup channels is important.

In the right panel of Fig. 4, the dashed line is the result including the  $\ell = 0, 1,$  and 2 breakup continua with  $\Delta_k = 0.01 \text{ fm}^{-1}$  and  $k_{\text{max}} = 2.0 \text{ fm}^{-1}$  ( $N_{\text{ch}} = 1201$ ), and the dotted line is the result including the  $\ell = 0, 1, 2, 3, 4,$  and 5 breakup continua with  $\Delta_k = 0.02 \text{ fm}^{-1}$  and  $k_{\text{max}} = 2.0 \text{ fm}^{-1}$  ( $N_{\text{ch}} = 2101$ ). The dashed and solid lines both agree well with the solid line, which is the same as in Fig. 3. In fact, the resulting values of  $(C_{\alpha^{13}\text{C}}^{17\text{O}^*})^2$  differ from each other by less than 1%. Thus, the modelspace used in the solid line of Fig. 3 gives good convergence of the calculated cross section, hence  $C_{\alpha^{13}\text{C}}^{17\text{O}^*}$ .

### 3.5. Discussion on the comparison with the previous DWBA analysis

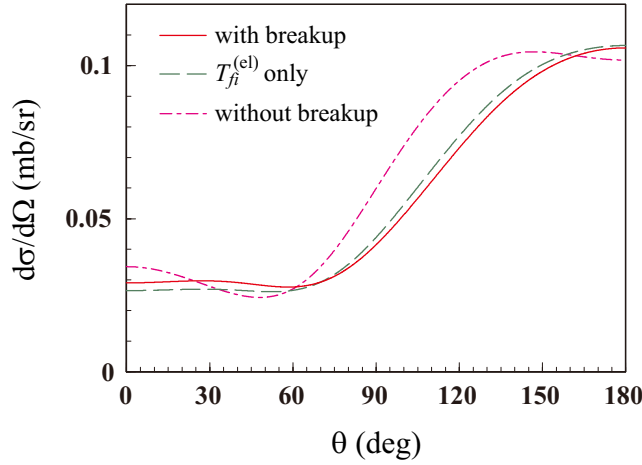


Fig. 5. (color online)  ${}^6\text{Li}$ -breakup effect on the transfer reaction  ${}^{13}\text{C}({}^6\text{Li}, d){}^{17}\text{O}^*$  at 3.6 MeV. The solid and dash-dotted lines show the results of calculations with and without  ${}^6\text{Li}$  breakup channels, respectively. The dashed line stands for the result of the elastic transfer process only. The solid and dash-dotted lines are respectively the same as those in the right panel of Fig. 4.

Figure 5 shows the  ${}^6\text{Li}$ -breakup effect on the transfer reaction. The solid and dash-dotted lines are the results of the calculation with and without the breakup channels, respectively; they are shown also in the right panel of Fig. 4. The two results largely deviate from each other, indicating that the breakup effect is important, as mentioned in §3.4. This does not necessarily mean, however, inadequacy of DWBA, as discussed below. The transition matrix elements of the transfer reaction can be separated into two parts,

$$T_{fi} = S_{\text{exp}}^{1/2} \left[ T_{fi}^{(\text{el})} + T_{fi}^{(\text{br})} \right] \quad (3.9)$$

with

$$T_{fi}^{(\text{el})} = \langle \Psi_f^{(-)} | V_{\text{tr}} | \Psi_{\text{el}}^{(+)} \rangle, \quad (3.10)$$

$$T_{fi}^{(\text{br})} = \langle \Psi_f^{(-)} | V_{\text{tr}} | \Psi_{\text{br}}^{(+)} \rangle, \quad (3.11)$$

where  $\Psi_{\text{el}}^{(+)}$  and  $\Psi_{\text{br}}^{(+)}$  are the elastic and breakup parts of the CDCC wave function  $\Psi_i^{\text{CDCC}}$ . The transition matrix  $T_{fi}^{(\text{el})}$  describes the transfer reaction from the elastic channel, i.e., the elastic transfer process, which includes the back-coupling effect of the breakup channels to the elastic channel. On the other hand,  $T_{fi}^{(\text{br})}$  describes the transfer reaction from  ${}^6\text{Li}$  breakup channels, i.e., the breakup transfer process. Thus, there are two kinds of breakup effects on the transfer reaction; one is the back-coupling effect in the elastic transfer process and the other is the presence of the breakup transfer process. The dashed line is a result of the elastic transfer transition only. The result agrees with the solid line, indicating that the breakup transfer transition is much smaller than the elastic transfer one. This is consistent with the small breakup cross section of  ${}^6\text{Li}$  by  ${}^{13}\text{C}$  as mentioned in §3.2. Hence, only the back-coupling effect is important in the present subbarrier transfer reaction. In DWBA, the back-coupling effect is expected to be included by using the  ${}^6\text{Li}$  optical potential, which describes the elastic scattering by definition, as the distorting potential. The ANC,  $(C_{\alpha^{13}\text{C}}^{17\text{O}^*})^2$ , extracted in the preceding DWBA calculation<sup>2)</sup> is  $0.89 \pm 0.23 \text{ fm}^{-1}$ . This value agrees well with the present result Eq. (3.8) within the uncertainties.

#### §4. Summary

In summary, we analyze the  ${}^{13}\text{C}({}^6\text{Li}, d){}^{17}\text{O}(6.356 \text{ MeV}, 1/2^+)$  reaction at 3.6 MeV by the three-body ( $\alpha + d + {}^{13}\text{C}$ ) model. The breakup effects of  ${}^6\text{Li}$  and  ${}^{17}\text{O}$  are investigated by CDCC. Those of  ${}^6\text{Li}$  are found important as a large back-coupling to the elastic channel, while those of  ${}^{17}\text{O}$  turns out negligible with an error of 5%. The transfer cross section is calculated with Born approximation to the transition interaction, and including only the breakup of  ${}^6\text{Li}$ . The ANC extracted by the three-body reaction model is  $(C_{\alpha^{13}\text{C}}^{17\text{O}^*})^2 = 1.03 \pm 0.25$  (theor)  $\pm 0.15$  (expt). The back-coupling effect of  ${}^6\text{Li}$  breakup on the transfer reaction is large, while the breakup transfer transition is negligible compared with the elastic transfer transition. The preceding DWBA calculation implicitly treated the back-coupling effect by using a  ${}^6\text{Li}$  optical potential that described the elastic scattering as the distorting potential. The value of  $(C_{\alpha^{13}\text{C}}^{17\text{O}^*})^2$  extracted by DWBA is  $0.89 \pm 0.23 \text{ fm}^{-1}$ , which is consistent with the present value within the uncertainties. It can be conjectured that in the DWBA calculation, the aforementioned back-coupling effect in the initial channel was properly included. However, this will not always be the case, since the optical potential is determined phenomenologically. Furthermore, breakup transfer processes may be important in other subbarrier  $\alpha$  transfer reactions. The present three-body approach, therefore, should be applied systematically to these reactions. From theoretical point of view, inclusion of CDCC wave functions in both initial and final channels will be an important subject; to achieve this, one should treat, in principle, very large coordinate space in the calculation of the  $T$  matrix, since there is no damping in the overlap kernel. It will be interesting to use four-body CDCC<sup>15)</sup> based on a  $p + n + \alpha + {}^{13}\text{C}$  model to obtain the wave function in the initial channel. At this stage, however, the modelspace required is too large for four-body CDCC to be applied.

One of the authors (K. O.) wishes to thank G. V. Rogachev and E. D. Johnson for valuable discussions and providing detailed information on their DWBA calculation. The authors are grateful to Y. Iseri for providing a computer code RANA for calculation of transfer processes. The computation was carried out using the computer facilities at the Research Institute for Information Technology, Kyushu University.

#### References

- 1) G. R. Satchler, *Direct Nuclear Reactions* (1983).
- 2) E. D. Johnson *et al.*, Phys. Rev. Lett. **97** (2006), 192701.
- 3) E. D. Johnson, G. V. Rogachev, J. Mitchell, and K. W. Kemper, Phys. Rev. C **80** (2009), 045805.
- 4) I. Iben, Astrophys. J. **196** (1975), 525.
- 5) A. M. Mukhamedzhanov and R. E. Tribble, Phys. Rev. C **59** (1999), 3418.
- 6) M. Kamimura, M. Yahiro, Y. Iseri, Y. Sakuragi, H. Kameyama, and M. Kawai, Prog. Theor. Phys. Suppl. No. 89 (1986), 1.
- 7) N. Austern, Y. Iseri, M. Kamimura, M. Kawai, G. Rawitscher and M. Yahiro, Phys. Rep. **154** (1987), 125.
- 8) K. Ogata, M. Yahiro, Y. Iseri, and M. Kamimura, Phys. Rev. C **67** (2003), 011602(R).
- 9) K. Ogata, S. Hashimoto, Y. Iseri, M. Kamimura, and M. Yahiro, Phys. Rev. C **73** (2006), 024605.
- 10) N. Austern, M. Yahiro and M. Kawai, Phys. Rev. Lett. **63** (1989), 2649.
- 11) N. Austern, M. Kawai and M. Yahiro, Phys. Rev. C **53** (1996), 314.
- 12) R. A. D. Piyadasa, M. Yahiro, M. Kamimura and M. Kawai, Prog. Theor. Phys. **81** (1989), 910.
- 13) Y. Sakuragi, M. Yahiro, and M. Kamimura, Prog. Theor. Phys. Suppl. No. 89 (1986), 136.
- 14) T. Matsumoto, T. Kamizato, K. Ogata, Y. Iseri, E. Hiyama, M. Kamimura, and M. Yahiro, Phys. Rev. C **68** (2003), 064607.
- 15) T. Matsumoto, T. Egami, K. Ogata, Y. Iseri, M. Kamimura, and M. Yahiro, Phys. Rev. C **73** (2006), 051602(R).